AGU PUBLICATIONS

Geophysical Research Letters

RESEARCH LETTER
10.1002/2016GL071206

Key Points:
- A new possible aerosol effect on the tropical circulation and rain patterns is proposed
- Aerosol loading increases water vapor content in the environment of trade wind clouds due to a suppression of precipitation
- A decrease in subtropical precipitation in a GCM results in intensification of the equatorial precipitation and Hadley circulation

Supporting Information:
- Supporting Information S1

Correspondence to:
G. Dagan,
guy.dagan@weizmann.ac.il

Citation:
Dagan, G., and R. Chemke (2016), The effect of subtropical aerosol loading on equatorial precipitation, *Geophys. Res. Lett.*, *43*, 11,048–11,056, doi:10.1002/2016GL071206.

Received 2 AUG 2016
Accepted 28 SEP 2016
Accepted article online 3 OCT 2016
Published online 30 OCT 2016

©2016. American Geophysical Union. All Rights Reserved.

The effect of subtropical aerosol loading on equatorial precipitation

G. Dagan[1] and R. Chemke[1]

[1]Department of Earth and Planetary Sciences, Weizmann institute of Science, Rehovot, Israel

Abstract Cloud-aerosol interactions are considered as one of the largest sources of uncertainties in the study of climate change. Here another possible cloud-aerosol effect on climate is proposed. A series of large eddy simulations (LES) with bin microphysics reveal a sensitivity of the total atmospheric water vapor amount to aerosol concentration. Under polluted conditions the rain is suppressed and the total amount of water vapor in the atmosphere increases with time compared to clean precipitating conditions. Theoretical examination of this aerosol effect on water vapor transport from the subtropics to the tropics, and hence on the equatorial rain and Hadley circulation, is conducted using an idealized general circulation model (GCM). It is shown that a reduction in the subtropical rain amount results in increased water vapor advection to the tropics and enhanced equatorial rain and Hadley circulation. This joins previously proposed mechanisms on the radiative aerosol effect on the general circulation.

1. Introduction

Changes in aerosol concentration, which acts as cloud condensation nuclei (CCNs), modulate the cloud droplet concentration and size distribution. Liquid (warm) clouds forming under high aerosol loading (polluted conditions) will initially have smaller and more numerous droplets, with narrower size distributions compared to clouds forming under clean conditions [*Fitzgerald and Spyers-Duran*, 1973; *Squires*, 1958; *Squires and Twomey*, 1960; *Warner and Twomey*, 1967].

The initial droplet size distribution affects key cloud processes such as condensation-evaporation, collision-coalescence, and sedimentation. More specifically, the initiation of collision-coalescence is delayed with increasing aerosol loading [*Albrecht*, 1989; *Gunn and Phillips*, 1957; *Squires*, 1958]. This further drives a delay in rain formation and can affect the surface rain amount [*Dagan et al*., 2015a, 2015b; *Fan et al*., 2007; *Khain*, 2009; *Koren et al*., 2012; *Levin and Cotton*, 2009; *Rosenfeld*, 1999, 2000]. Under low aerosol concentration, an increase in aerosol loading may result in intensification of the rain rates and total amount from warm convective clouds [*Dagan et al*., 2015a, 2015b; *Koren et al*., 2014]. This trend continues up to an optimal aerosol concentration (N_{op}) that yields the maximum rain per given thermodynamic conditions. For concentrations above N_{op}, the aerosols enhance mixing with the noncloudy drier air [*Jiang et al*., 2006; *Small et al*., 2009; *Xue and Feingold*, 2006] and the enhanced accumulated water loading, due to the delay in rain initiation (which has a negative effect on the buoyancy) [*Dagan et al*., 2015a], suppresses cloud development. N_{op} is a function of the thermodynamic conditions such that conditions that support larger clouds also dictate larger N_{op} values.

For trade wind convective clouds (relatively small clouds) the N_{op} for rain is around 25 cm^{-3} [*Dagan et al*., 2015a, 2016a], and hence, under typical aerosol conditions, an increase in aerosol loading will result in rain suppression. Warm rain suppression with increasing aerosol loading was shown before, by both observations and numerical studies, for a large range of aerosol and meteorological conditions [*Altaratz et al*., 2008; *Jiang et al*., 2006; *Rosenfeld*, 1999, 2000; *Seigel*, 2014; *Xue and Feingold*, 2006; *Xue et al*., 2008]. These warm clouds are frequent over the oceans [*Norris*, 1998] and play an important role in the boundary layer's energy and moisture budgets. In addition, they are crucial for feeding deep convection systems in the tropics and are responsible for the largest uncertainty in tropical cloud feedback in climate models [*Bony and Dufresne*, 2005].

Clouds affect their surrounding thermodynamic conditions [*Heus and Jonker*, 2008; *Johnson et al*., 2002; *Lee et al*., 2014; *Roesner et al*., 1990; *Starr Malkus*, 1954; *Zhao and Austin*, 2005; *Zuidema et al*., 2012] (G. Dagan et al., Aerosol effect on the evolution of the thermodynamic properties of warm convective cloud fields, *Scientific Reports*, in review, 2016b). Each generation of clouds modulates the environmental conditions in

which the next generation of clouds will develop. Previous studies showed that clouds act to moisten the upper part of the cloudy layer and to raise the inversion base height. This mechanism is referred to as "cloud deepening" [*Roesner et al*., 1990; *Stevens*, 2007; *Stevens and Seifert*, 2008; *Stevens and Feingold*, 2009], and its magnitude was shown to depend on the microphysical properties of the clouds [*Saleeby et al*., 2015; *Seifert et al*., 2015; *Stevens and Feingold*, 2009] (G. Dagan et al., in review, 2016b). On the same note, the role of warm convective clouds in moistening the free troposphere was shown to be important by using both observational data and cloud field numerical simulations [*Brown and Zhang*, 1997; *Holloway and Neelin*, 2009; *Johnson et al*., 1999; *Randall et al*., 2003; *Takemi et al*., 2004; *Waite and Khouider*, 2010]. Theoretical calculations demonstrate that even low rain rates can significantly affect the thermodynamic properties of the boundary layer at trade wind regions [*Albrecht*, 1993]. Latent heat release and the removal of water by precipitation drive warmer, drier, shallower, and more stable cloudy layer compared to nonprecipitation conditions [*Albrecht*, 1993].

From a global perspective, it was shown that the direct (absorbing or scattering) and indirect (via effects on clouds) aerosol radiative forcing could alter the atmospheric circulation and hence the global precipitation patterns. Recently, it was shown that changes in the distribution of precipitation with respect to preindustrial era are largely dominated by aerosols [*Wang*, 2015; *Wu et al*., 2013]. The asymmetrical aerosol emissions between the northern and southern hemispheres may lead to a shift in the location of the Intertropical Convergence Zone (ITCZ) [cf. *Lucas et al*., 2014; *Schneider et al*., 2014]. Aerosols were proposed to cause a shift in the ITCZ's mean location toward the southern hemisphere [*Ramaswamy and Chen*, 1997; *Rotstayn and Lohmann*, 2002], due to cooling of the northern hemisphere by enhancing cloud albedo [*Twomey*, 1977] or scattering. On the other hand, increased concentrations of absorbing aerosols in the northern hemisphere may lead to a northward migration of the ITCZ [*Wang*, 2004]. In addition to the above anthropogenic aerosol effect, an increase in greenhouse gases concentrations can modulate the global hydrological cycle and rain patterns as well [*Allen and Ingram*, 2002; *Held and Soden*, 2006; *Zhang et al*., 2007].

As warm convective trade wind clouds play a crucial role in moisture processes in the subtropics and are part of the Hadley circulation, the aerosol's effect on these clouds and thus, on the dynamics of the tropical hydrological cycle, is studied. Here, in order to isolate the aerosol's thermodynamic effect on the large-scale circulation, their previously found radiative effects (absorbing and scattering) on the tropical circulation are missing. Using a large eddy simulation (LES) model with a detailed bin-microphysics scheme (section 2.1) and an idealized GCM (section 2.2) the coupled microphysical-dynamic system on a cloud field and on the global scales are explored. This further elucidates how changes driven by the coupling between microphysics and dynamics in small scales propagate and affect the way by which clouds change their environment and may even affect the general circulation and rain patterns in the tropics.

2. Materials and Methods

2.1. LES

The System for Atmospheric Modeling (SAM), nonhydrostatic, anelastic LES model version 6.10.3 [*Khairoutdinov and Randall*, 2003] is used to simulate the trade cumulus case of Barbados Oceanographic and Meteorological Experiment (BOMEX) [*Holland and Rasmusson*, 1973; *Siebesma et al*., 2003]. This case is based on observations made near Barbados during June 1969 and was initialized using the setup specified in *Siebesma et al*. [2003]. The setup includes surface fluxes and large-scale forcing [cf. *Heiblum et al*., 2016a]. The horizontal resolution is set to 100 m, while the vertical resolution is set to 40 m. The domain size is $12.8 \times 12.8 \times 4.0\ \mathrm{km}^3$, and the time step is 1 s. The model runs for 16 h.

A bin microphysical scheme [*Khain and Pokrovsky*, 2004] is used, which solves warm microphysical processes, including droplet nucleation, diffusional growth, collision coalescence, sedimentation, and breakup.

The aerosol distribution is based on marine aerosol size distribution [*Jaenicke*, 1988]. Eight different simulations are conducted with different aerosol concentration in the range of 5–5000 cm^{-3} [*Dagan et al*., 2015a]. To avoid giant CCN effects (that were shown to be able to produce rain even under polluted conditions [*Dagan et al*., 2015b; *Feingold et al*., 1999; *Yin et al*., 2000]), aerosols above 2 μm are cut off from the distribution. The smallest aerosol bin used is 5 nm. The water drop bin radii range between 2 μm and 3.2 mm. For both aerosol and water species, successive bins represent doubling of mass.

2.2. Idealized GCM

2.2.1. Model Description

An idealized moist GCM is used to study the effect of subtropical rain and moisture variations on the large-scale circulation and precipitation patterns. The model is based on the Geophysical Fluid Dynamics Laboratory flexible model system and solves the primitive equations on a sphere [*Frierson et al.*, 2006]. The model has an ocean slab at the lower boundary, with no topography. The ocean slab has no dynamics and only exchanges heat and moisture with the lowest atmospheric level. A constant perpetual equinox solar flux is imposed at the top of the atmosphere, which exponentially decays in the atmosphere and is reflected at the surface with a constant planetary albedo. The longwave radiation is parameterized using a two-stream gray radiation scheme and is a function of latitude and pressure [*Goody*, 1964; *Held*, 1982].

Water vapor is advected in the model and removed by convection and large-scale condensation. The convection scheme acts to relax the temperature toward a moist adiabatic lapse rate with a time scale of 2 h and the water vapor toward a profile of 70% relative humidity relative to the moist adiabatic lapse rate [*Betts and Miller*, 1986; *Betts*, 1986]. By precipitating condensed water, the large-scale condensation prevents the specific humidity to exceed saturation. Vapor saturation is calculated using the Clausius-Clapeyron relation:

$$e_s = \alpha e_0 exp\left(-\frac{L_v}{R_v}\left(\frac{1}{T}-\frac{1}{T_0}\right)\right), \tag{1}$$

where α is a rescaling parameter with a reference value $\alpha = 1$, $e_0 = 610.78$ Pa, $L_v = 2.5 \times 10^6$ J kg^{-1} is the latent heat release of vaporization, $R_v = 651.5$ J kg^{-1} K^{-1} is the gas constant for water, T is the temperature, and $T_0 = 273.16$°C. To include the effect of moisture on density, the model uses the virtual temperature.

2.2.2. Simulations Setup

Similar to *Frierson et al.* [2006], for simulating changes of atmospheric water vapor content and precipitation in the subtropics (due to changes in aerosol properties) the α parameter in equation (1) is varied between 0.8 and 1.35. This is done at latitude 12°N (the location of the subtropical minimum precipitation; Figure 2b) and exponentially decays or grows both poleward and equatorward to 1, such that it resides within the subtropics (Figure S1 in the supporting information). The equatorial region (deep tropics) is defined, following *Byrne and Schneider* [2016], from the ascending branch of the Hadley cell (where the mean meridional mass stream function is zero) to the closest latitude poleward where the mean meridional mass stream function reaches a local maximum (i.e., where its meridional gradient is zero). Using this definition, through all simulations the equatorial region spans between the equator and ~6.6°N (Figure 3). The subtropical region is defined from the edge of the tropical region to the edge of the Hadley cell (the latitude where the stream function changes sign at the height of its maximum value, ~25°N; Figure 3b) [*Walker and Schneider*, 2006]. For consistency with the LES simulations and observations (Figure S2) [*Platnick et al.*, 2003; *Dee et al.*, 2011], the maximum and minimum values of α are chosen to represent maximum changes of up to 20% in specific humidity. The reference simulation ($\alpha = 1$) represents Earth-like climate, with mean temperature and zonal wind fields similar to observations (Figure S3). Lower (higher) values of α decrease (increase) the amount of water vapor needed for saturation and thus increase (decrease) the precipitation and decrease (increase) the atmospheric water vapor content. As the model is axis symmetric, this is done only in the northern hemisphere's subtropics for comparison purposes and for representing the asymmetrical nature of anthropogenic aerosol emission. The model runs with 30 vertical sigma layers (pressure normalized by surface pressure) and T170 (0.7×0.7°) horizontal and 6 h time resolutions. Each simulation is integrated over 1500 days to ensure that steady state is reached, and the results represent the last 500 days.

The model is idealized in that it lacks, for example, the seasonal and diurnal cycles, chemistry processes, land, and clouds. Thus, this model does not capture the exact moisture and precipitation contents of the observed atmosphere. However, its idealization enables isolating and understanding the dynamical and thermodynamic behaviors of the atmosphere in a realistic framework. Moreover, the representation of the aerosol's effects on warm convective clouds in the GCM simulations is simplistic and focuses only on one aspect (a decrease in precipitation due to an increase in aerosol loading). While this simplistic approach prevents investigating the full feedback between aerosols and the general circulation, it enables isolating the thermodynamic effect on the general circulation from other effects and feedback (e.g., aerosol radiative effects).

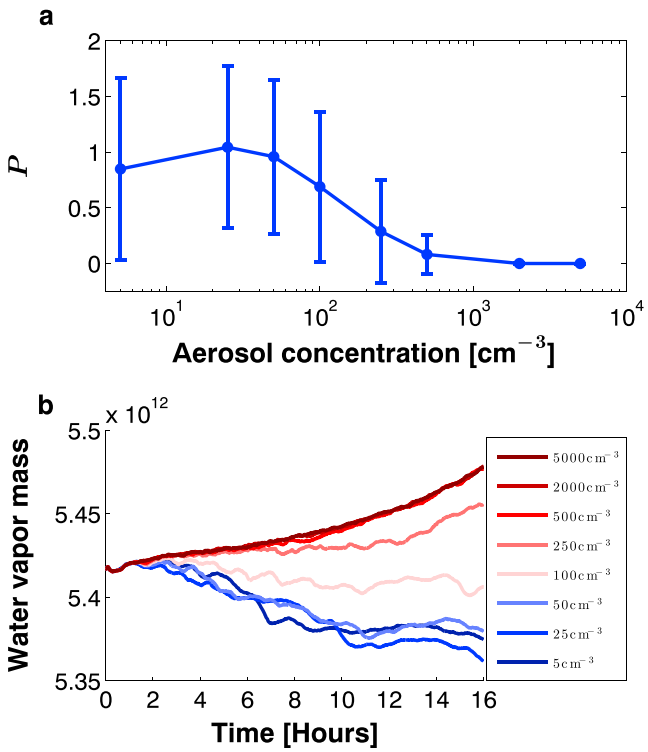

Figure 1. (a) Time (excluding the first 2 h of simulation) and domain mean rain rate (mm d^{-1}) as a function of the aerosol loading (vertical lines represent the standard deviations). (b) Total water vapor mass in the domain (g) as a function of time for different aerosol loading levels. Each color corresponds to a different aerosol concentration; warmer (colder) colors correspond to polluted (pristine) conditions.

3. Results

3.1. The Aerosol Effect on Trade Wind Clouds in LES Domain

Under extremely clean conditions there is an increase in rain rate with aerosol loading (~23% increase between 5 and 25 cm^{-3}; Figure 1a) [*Dagan et al.*, 2015a, 2015b, 2016a]. This increase is a result of an increase in the condensation efficiency with aerosol loading, which enhances development of those aerosol limited clouds [*Koren et al.*, 2014]. Moreover, the droplets' mobility in the air increases with aerosol loading, which causes the smaller droplets in more polluted clouds to be pushed higher in the atmosphere and promote cloud development [*Koren et al.*, 2015]. In agreement with previous numerical studies [*Heiblum et al.*, 2016b; *Jiang and Feingold*, 2006; *Seigel*, 2014; *Xue et al.*, 2008], an additional increase in aerosol loading results in a decrease in rain rate (P) from warm convective cloud fields (from 1.05 mm/d for the simulation with aerosol concentration of 25 cm^{-3} down to 0 for simulations with aerosol concentration of ≥2000 cm^{-3}; Figure 1a). This decrease is a result of the enhanced evaporation and mixing at the cloud margin [*Small et al.*, 2009] and the enhanced water loading effect due to the delayed precipitation [*Dagan et al.*, 2015a, 2016a].

By changing the clouds' and rain's properties, aerosols may affect the moisture (and temperature) vertical profile [*Albrecht*, 1993] (G. Dagan et al., in review, 2016b). The absence of rain from the polluted clouds results in a net condensation in the lower cloudy layer and a net evaporation at the upper cloudy and inversion layers. This dipole pattern of condensational heating below and evaporative cooling above, under polluted conditions, results in an increase in the thermodynamic instability and moistening of the upper cloudy and inversion layers [*Dagan et al.*, 2016a] (G. Dagan et al., in review, 2016b). On the other hand, under clean precipitating conditions, the net condensation in the cloudy layer and net evaporation at the subcloud layer results in stabilization of the profile (consumption of the thermodynamic instability) and drying of the cloudy layer [*Albrecht*, 1993] (G. Dagan et al., in review, 2016b).

Thus, changes in the vertical thermodynamic conditions due to aerosol loading, are accompanied with changes in the total amount of water vapor in the atmosphere. Figure 1b shows the total water vapor mass

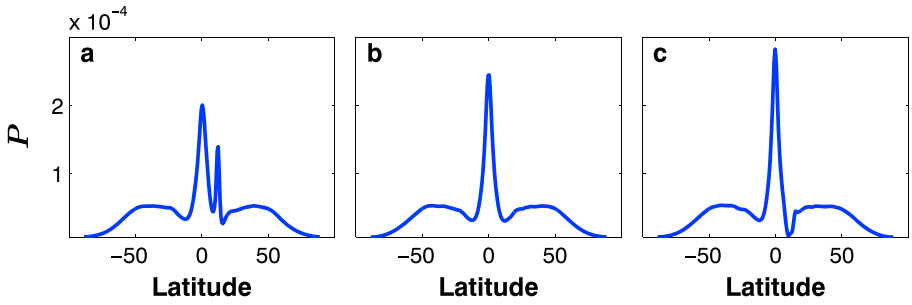

Figure 2. Zonal and time mean precipitation intensity (kg m^{-2} s^{-1}) as a function of latitude for three simulations of (a) $\alpha = 0.8$, (b) $\alpha = 1$, and (c) $\alpha = 1.2$.

in the domain as a function of time for all eight simulations differ by the aerosol loading. Indeed, for the polluted simulations (250 cm^{-3} and above) the total water vapor mass increases with time, while for the clean simulations (100 cm^{-3} and below) it decreases.

In a recent work, *Seifert et al.* [2015] proposed that due to a "buffering" [*Stevens and Feingold*, 2009] of the aerosol effects on clouds, the cloud field may reach an "equilibrium state" after a few tens of hours. In this state, the aerosols do not play an important role in setting the domain's rain amount, cloud fraction, and cloud radiative forcing. However, even under this equilibrium state, the moisture and temperature profiles are not expected to be similar under clean and polluted conditions [*Seifert et al.*, 2015].

3.2. The Effect of Subtropical Moisture on the Tropical Circulation

To further examine the effects of an increase in atmospheric water vapor content in the subtropics on the rain patterns and the tropical circulation in the atmosphere, a series of idealized GCM simulations are conducted, with different subtropical precipitation intensity and water vapor content. The amounts of precipitation and water vapor in the northern hemisphere subtropics are varied, through a control parameter (α) in the Clausius-Clapeyron relation (section 2.2), which mimics the aerosol effect found in the LES simulations (Figure 1b).

The Hadley cell circulation results in maximum precipitation at the equator, due to the convergence of the equatorward moist air at the surface, and in minimum value in the subtropics where the dry air descends (Figures 2b, 3b, and S3b). In Figure 4 the zonal and time mean equatorial and subtropical (cf. section 2.2.2 for definitions) precipitation intensity and meridional moisture fluxes are shown relative to the reference simulation ($\alpha = 1$). The meridional moisture fluxes are vertically averaged from the surface to 800 mb, for accounting only their near-surface values in the returning branch of the Hadley cell.

At values of α below one, a smaller amount of water vapor is needed to reach saturation. Thus, the equatorward moving air near the surface accumulates enough moisture to reach condensation and thus precipitate even before reaching the equator (Figures 2a and 4a (red dots)—mimicking low aerosol concentrations). This further decreases the equatorial precipitation intensity due to weaker moisture fluxes to the equator (blue dots in Figure 4b). For a 0.2 decrease in α (i.e., ~10% decrease in subtropical specific humidity) the equatorial

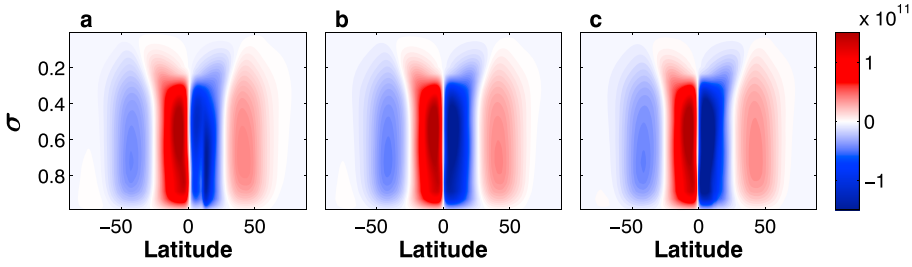

Figure 3. Zonal and time mean meridional mass stream function (kg s^{-1}) as a function of sigma and latitude for (a) $\alpha = 0.8$, (b) $\alpha = 1$, and (c) $\alpha = 1.2$. The blue and red colors represent the clockwise and counterclockwise circulations, respectively.

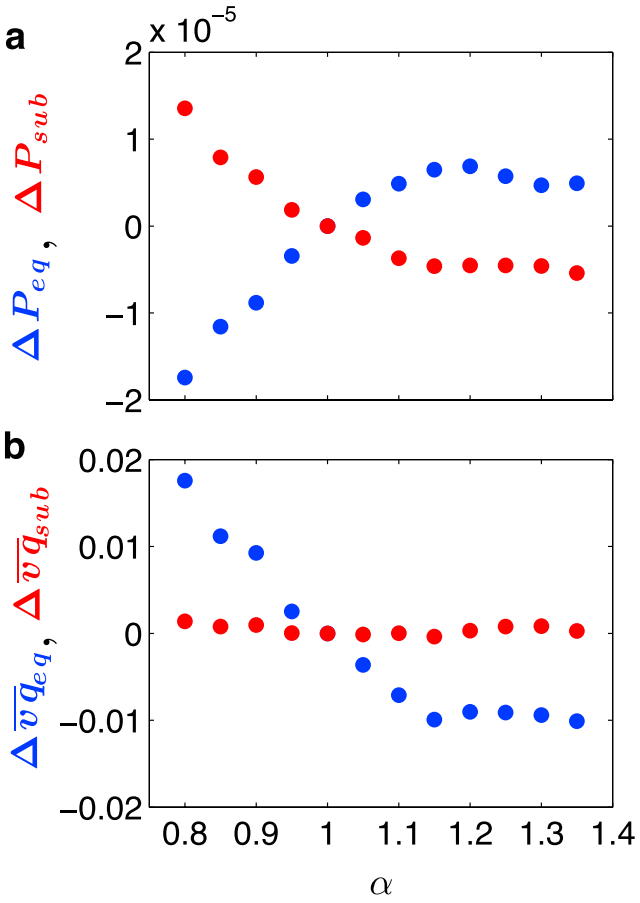

Figure 4. (a) Zonal and time mean equatorial (blue) and subtropical (red) precipitation intensity (kg m^{-2} s^{-1}) as a function of α, relative to the reference simulation ($\alpha = 1$). (b) Zonal and time mean equatorial (blue) and subtropical (red) near-surface meridional moisture fluxes (kg kg^{-1} m s^{-1}) as a function of α, relative to the reference simulation ($\alpha = 1$).

precipitation decreases by ~12% and the moisture fluxes by ~65%. As the moisture fluxes in the returning branch of the northern hemisphere's Hadley cell are negative (i.e., southward; Figure S3b), a positive value in Figure 4b indicates weaker fluxes than in the reference simulation. At values of α above one, the high amount of water vapor needed to reach saturation suppresses precipitation in the subtropics (Figures 2c and 4a (red dots)—mimicking high aerosol concentrations). This enables a larger amount of moisture to reach the equator (blue dots in Figure 4b) and to increase its precipitation (Figures 2c and 4a (blue dots)). For a 0.2 increase in α (i.e., ~10% increase in subtropical specific humidity) the subtropical precipitation decreases by ~11%, and the moisture fluxes and equatorial precipitation increase by ~35% and ~5%, respectively. This behavior is similar to the "wet-get-wetter, dry-get-drier" response in warmer climates, where the amount of water vapor in the atmosphere is increased based on equation (1) [*Held and Soden*, 2006]. Different than the radiative effect of aerosols [e.g., *Ramaswamy and Chen*, 1997; *Rotstayn and Lohmann*, 2002; *Wang*, 2004], here their effect on moisture processes does not shift the ITCZ off the equator but only changes its intensity.

Changes in equatorial condensation and precipitation intensity affect the strength of the Hadley circulation, through changes in latent heat release. As rain is suppressed in the subtropics (high aerosol concentrations), the large equatorward moisture fluxes result in stronger equatorial precipitation and latent heat release, which further strengthens the ascending branch of the Hadley cell up to 20% (when α is increased by 0.2; Figure 3c). This results in a positive feedback, as stronger Hadley circulation further suppresses subtropical precipitation. On the other hand, at values of α below one (low aerosol concentrations), the increased rain amount at latitudes poleward of the equator results in a secondary direct circulation in these latitudes (corresponding to the double precipitation maxima; Figure 2a), which weakens the ascending branch of the Hadley cell at the equator and the overall circulation by 20% in the most extreme case ($\alpha = 0.8$; Figure 3a). Again, the Hadley circulation acts as a positive feedback, as it further enables an increase in subtropical precipitation.

Interestingly, above a threshold value of $\alpha = 1.15$, the moisture fluxes and precipitation trends reach saturation, as the subtropical precipitation is entirely suppressed (Figure 4a). Thus, further suppressing condensation of water vapor (by increasing α) results in a similar meridional flux of water vapor toward the equator (blue dots in Figure 4b). Different than the meridional moisture flux to the equator, the moisture flux in the subtropics remains constant, regardless of the amount of moisture (red dots in Figure 3b). This occurs as an increase (decrease) of moisture flux toward the equator is compensated by an increase (decrease) of moisture flux to the subtropical region from higher latitudes (not shown).

4. Summary

A possible aerosol effect on the tropical circulation of the atmosphere and rain patterns is proposed. It is shown using LES simulations with a detailed bin microphysics that an increase in aerosol loading in subtropical trade wind clouds results in a decrease in precipitation and an increase in total water vapor amount in the atmosphere. Using idealized GCM simulations, it is shown that a decrease in precipitation and an increase in water vapor content in the subtropics is translated to an increase in the near-surface equatorward moisture fluxes of the Hadley cell. As a result, equatorial precipitation at the ascending branch of the Hadley cell increases. Moreover, the increased equatorward moisture fluxes result in an intensification of the Hadley circulation, which further suppress (enhance) subtropical (equatorial) precipitation.

Although the spatial and temporal scales and, in many cases, the underline physics are different, it is worth mentioning the similarity between the aerosols' effect found in this study and studies focusing on different scales. Initial rain suppression by aerosol with a compensation later on was reported in a single cloud scale [e.g., *Altaratz et al*., 2008; *Rosenfeld et al*., 2008], as well as in regional orographic scales [e.g., *Cotton et al*., 2010; *Givati and Rosenfeld*, 2004, 2005; *Rosenfeld and Givati*, 2006; *Yang et al*., 2013].

Previous studies proposed that via a direct (absorbing or scattering) or an indirect (effects on clouds) radiative forcing, aerosol can affect the general circulation and shift the global rain patterns southward [e.g., *Rotstayn and Lohmann*, 2002] or northward [*Wang*, 2004]. Here on the other hand, it is proposed that by modulating the rain and atmospheric moisture, aerosol can affect the general tropical circulation and intensify equatorial precipitation, with no corresponding poleward shift.

Moreover, aerosols were also shown to affect rain amounts from deep convective clouds in the tropics [*Fan et al*., 2007; *Khain*, 2009; *Koren et al*., 2012; *Lee et al*., 2008; *Levin and Cotton*, 2009]. Specifically, aerosol loading was found to intensify precipitation near the equator [*Koren et al*., 2012]. This may further enhance the Hadley circulation, as demonstrated here for subtropical aerosol loading. Thus, the overall effect of aerosol loading in the tropics may result in stronger Hadley circulation, which strengthens the wet-get-wetter, dry-get-drier paradigm [*Held and Soden*, 2006].

In this study we used a hierarchy of model approach [*Held*, 2014], using LES and idealized GCM simulations. As these models are not online coupled, there is no feedback between them, which allows investigating only the end result of each effect. The GCM simulations are idealized and designed to only mimic the aerosol's effect seen in the LES simulations of reduced subtropical precipitation and increased atmospheric water vapor content. The proposed mechanism of the aerosol effect on the atmospheric general circulation should be further investigated using more sophisticated numerical models that include better representation of convective clouds and other feedbacks between aerosols and the general circulation.

Acknowledgments
We thank Ilan Koren and Yohai Kaspi for their helpful conversations during the preparation of this manuscript. Any additional data may be obtained from Guy Dagan (e-mail: guy.dagan@weizmann.ac.il).

References

Albrecht, B. A. (1989), Aerosols, cloud microphysics, and fractional cloudiness, *Science*, *245*(4923), 1227.
Albrecht, B. A. (1993), Effects of precipitation on the thermodynamic structure of the trade wind boundary layer, *J. Geophys. Res.*, *98*(D4), 7327–7337, doi:10.1029/93JD00027.
Allen, M. R., and W. J. Ingram (2002), Constraints on future changes in climate and the hydrologic cycle, *Nature*, *419*(6903), 224–232.
Altaratz, O., I. Koren, T. Reisin, A. Kostinski, G. Feingold, Z. Levin, and Y. Yin (2008), Aerosols' influence on the interplay between condensation, evaporation and rain in warm cumulus cloud, *Atmos. Chem. Phys.*, *8*(1), 15–24.
Betts, A. K. (1986), A new convective adjustment scheme. Part I: Observational and theoretical basis, *Q. J. R. Meteorol. Soc.*, *112*(473), 677–691.
Betts, A., and M. Miller (1986), A new convective adjustment scheme. Part II: Single column tests using GATE wave, BOMEX, ATEX and arctic air-mass data sets, *Q. J. R. Meteorol. Soc.*, *112*(473), 693–709.
Bony, S., and J. L. Dufresne (2005), Marine boundary layer clouds at the heart of tropical cloud feedback uncertainties in climate models, *Geophys. Res. Lett.*, *32*, L20806, doi:10.1029/2005GL023851.
Brown, R. G., and C. Zhang (1997), Variability of midtropospheric moisture and its effect on cloud-top height distribution during TOGA COARE*, *J. Atmos. Sci.*, *54*(23), 2760–2774.
Byrne, M. P., and T. Schneider (2016), Energetic constraints on the width of the Intertropical Convergence Zone, *J. Clim.*, doi:10.1175/JCLI-D-15-0767.1.
Cotton, W. R., D. Ward, and S. Saleeby (2010), Aerosol impacts on wintertime orographic precipitation, paper presented at 13th conference on Clouds Physics.
Dagan, G., I. Koren, and O. Altaratz (2015a), Competition between core and periphery-based processes in warm convective clouds—From invigoration to suppression, *Atmos. Chem. Phys.*, *15*(5), 2749–2760, doi:10.5194/acp-15-2749-2015.
Dagan, G., I. Koren, and O. Altaratz (2015b), Aerosol effects on the timing of warm rain processes, *Geophys. Res. Lett.*, *42*, 4590–4598, doi:10.1002/2015GL063839.
Dagan, G., I. Koren, O. Altaratz, and R. H. Heiblum (2016a), Time dependent, non-monotonic response of warm convective cloud fields to changes in aerosol loading, *Atmos. Chem. Phys. Discuss.*, *2016*, 1–21, doi:10.5194/acp-2016-736.

Dee, D., S. Uppala, A. Simmons, P. Berrisford, P. Poli, S. Kobayashi, U. Andrae, M. Balmaseda, G. Balsamo, and P. Bauer (2011), The ERA-Interim reanalysis: Configuration and performance of the data assimilation system, *Q. J. R. Meteorol. Soc.*, *137*(656), 553–597.
Fan, J., R. Zhang, G. Li, and W.-K. Tao (2007), Effects of aerosols and relative humidity on cumulus clouds, *J. Geophys. Res.*, *112*, D14204, doi:10.1029/2006JD008136.
Feingold, G., W. R. Cotton, S. M. Kreidenweis, and J. T. Davis (1999), The impact of giant cloud condensation nuclei on drizzle formation in stratocumulus: Implications for cloud radiative properties, *J. Atmos. Sci.*, *56*(24), 4100–4117.
Fitzgerald, J., and P. Spyers-Duran (1973), Changes in cloud nucleus concentration and cloud droplet size distribution associated with pollution from St. Louis, *J. Appl. Meteorol.*, *12*(3), 511–516.
Frierson, D. M., I. M. Held, and P. Zurita-Gotor (2006), A gray-radiation aquaplanet moist GCM. Part I: Static stability and eddy scale, *J. Atmos. Sci.*, *63*(10), 2548–2566.
Givati, A., and D. Rosenfeld (2004), Quantifying precipitation suppression due to air pollution, *J. Appl. Meteorol.*, *43*(7), 1038–1056.
Givati, A., and D. Rosenfeld (2005), Separation between cloud-seeding and air-pollution effects, *J. Appl. Meteorol.*, *44*(9), 1298–1314.
Goody, R. (1964), *Atmospheric Radiation, Vol. I, Theoretical Basis*, Oxford Univ. Press, Oxford.
Gunn, R., and B. Phillips (1957), An experimental investigation of the effect of air pollution on the initiation of rain, *J. Meteorol.*, *14*(3), 272–280.
Heiblum, R. H., O. Altaratz, I. Koren, G. Feingold, A. B. Kostinski, A. P. Khain, M. Ovchinnikov, E. Fredj, G. Dagan, and L. Pinto (2016a), Characterization of cumulus cloud fields using trajectories in the center of gravity versus water mass phase space: 1. Cloud tracking and phase space description, *J. Geophys. Res. Atmos.*, *121*, 6336–6355, doi:10.1002/2015JD024186.
Heiblum, R. H., O. Altaratz, I. Koren, G. Feingold, A. B. Kostinski, A. P. Khain, M. Ovchinnikov, E. Fredj, G. Dagan, and L. Pinto (2016b), Characterization of cumulus cloud fields using trajectories in the center of gravity versus water mass phase space: 2. Aerosol effects on warm convective clouds, *J. Geophys. Res. Atmos.*, *121*, 6356–6373, doi:10.1002/2015JD024193.
Held, I. (2014), Simplicity amid complexity, *Science*, *343*(6176), 1206–1207.
Held, I. M. (1982), On the height of the tropopause and the static stability of the troposphere, *J. Atmos. Sci.*, *39*(2), 412–417.
Held, I. M., and B. J. Soden (2006), Robust responses of the hydrological cycle to global warming, *J. Clim.*, *19*(21), 5686–5699.
Heus, T., and H. J. Jonker (2008), Subsiding shells around shallow cumulus clouds, *J. Atmos. Sci.*, *65*(3), 1003–1018.
Holland, J. Z., and E. M. Rasmusson (1973), Measurements of the atmospheric mass, energy, and momentum budgets over a 500-kilometer square of tropical ocean, *Mon. Weather Rev.*, *101*(1), 44–55.
Holloway, C. E., and J. D. Neelin (2009), Moisture vertical structure, column water vapor, and tropical deep convection, *J. Atmos. Sci.*, *66*(6), 1665–1683.
Jaenicke, R. (1988), Aerosol physics and chemistry, in *Meterology Landolt-Börnstein*, *New Ser.*, vol. 4b, edited by G. Fischer, pp. 391–457 , Springer, Berlin.
Jiang, H. L., and G. Feingold (2006), Effect of aerosol on warm convective clouds: Aerosol-cloud-surface flux feedbacks in a new coupled large eddy model, *J. Geophys. Res.*, *111*, D01202, doi:10.1029/2005JD006138.
Jiang, H., H. Xue, A. Teller, G. Feingold, and Z. Levin (2006), Aerosol effects on the lifetime of shallow cumulus, *Geophys. Res. Lett.*, *33*, L14806, doi:10.1029/2006GL026024.
Johnson, D. E., W. Tao, J. Simpson, and C. Sui (2002), A study of the response of deep tropical clouds to large-scale thermodynamic forcings. Part I: Modeling strategies and simulations of TOGA COARE convective systems, *J. Atmos. Sci.*, *59*(24), 3492–3518.
Johnson, R. H., T. M. Rickenbach, S. A. Rutledge, P. E. Ciesielski, and W. H. Schubert (1999), Trimodal characteristics of tropical convection, *J. Clim.*, *12*(8), 2397–2418.
Khain, A., and A. Pokrovsky (2004), Simulation of effects of atmospheric aerosols on deep turbulent convective clouds using a spectral microphysics mixed-phase cumulus cloud model. Part II: Sensitivity study, *J. Atmos. Sci.*, *61*(24), 2983–3001.
Khain, A. P. (2009), Notes on state-of-the-art investigations of aerosol effects on precipitation: A critical review, *Environ. Res. Lett.*, *4*(1, 015004).
Khairoutdinov, M. F., and D. A. Randall (2003), Cloud resolving modeling of the ARM summer 1997 IOP: Model formulation, results, uncertainties, and sensitivities, *J. Atmos. Sci.*, *60*(4), doi:10.1175/1520-0469(2003)060<0607:CRMOTA>2.0.CO;2.
Koren, I., O. Altaratz, L. A. Remer, G. Feingold, J. V. Martins, and R. H. Heiblum (2012), Aerosol-induced intensification of rain from the tropics to the mid-latitudes, *Nat. Geosci.*, doi:10.1038/ngeo1364.
Koren, I., G. Dagan, and O. Altaratz (2014), From aerosol-limited to invigoration of warm convective clouds, *Science*, *344*(6188), 1143–1146, doi:10.1126/science.1252595.
Koren, I., O. Altaratz, and G. Dagan (2015), Aerosol effect on the mobility of cloud droplets, *Environ. Res. Lett.*, *10*(10, 104011).
Lee, S. S., L. J. Donner, V. T. J. Phillips, and Y. Ming (2008), The dependence of aerosol effects on clouds and precipitation on cloud-system organization, shear and stability, *J. Geophys. Res.*, *113*, D16202, doi:10.1029/2007JD009224.
Lee, S. S., B.-G. Kim, C. Lee, S. S. Yum, and D. Posselt (2014), Effect of aerosol pollution on clouds and its dependence on precipitation intensity, *Clim. Dyn.*, *42*(3-4), 557–577.
Levin, Z., and W. R. Cotton (2009), *Aerosol Pollution Impact on Precipitation: A Scientific Review*, Springer, Netherlands.
Lucas, C., B. Timbal, and H. Nguyen (2014), The expanding tropics: A critical assessment of the observational and modeling studies, *Wiley Interdisc. Rev. Clim. Change*, *5*(1), 89–112.
Norris, J. R. (1998), Low cloud type over the ocean from surface observations. Part II: Geographical and seasonal variations, *J. Clim.*, *11*(3), 383–403.
Platnick, S., M. D. King, S. A. Ackerman, W. P. Menzel, B. A. Baum, J. C. Riedi, and R. A. Frey (2003), The MODIS cloud products: Algorithms and examples from Terra, *IEEE Trans. Geosc. Remote Sens.*, *41*(2), 459–473.
Ramaswamy, V., and C. T. Chen (1997), Linear additivity of climate response for combined albedo and greenhouse perturbations, *Geophys. Res. Lett.*, *24*(5), 567–570, doi:10.1029/97GL00248.
Randall, D., M. Khairoutdinov, A. Arakawa, and W. Grabowski (2003), Breaking the cloud parameterization deadlock, *Bull. Am. Meteorol. Soc.*, *84*(11), 1547.
Roesner, S., A. Flossmann, and H. Pruppacher (1990), The effect on the evolution of the drop spectrum in clouds of the preconditioning of air by successive convective elements, *Q. J. R. Meteorol. Soc.*, *116*(496), 1389–1403.
Rosenfeld, D. (1999), TRMM observed first direct evidence of smoke from forest fires inhibiting rainfall, *Geophys. Res. Lett.*, *26*(20), 3105–3108, doi:10.1029/1999GL006066.
Rosenfeld, D. (2000), Suppression of rain and snow by urban and industrial air pollution, *Science*, *287*(5459), 1793–1796.
Rosenfeld, D., and A. Givati (2006), Evidence of orographic precipitation suppression by air pollution-induced aerosols in the western United States, *J. Appl. Meteorol. Climatol.*, *45*(7), 893–911.
Rosenfeld, D., U. Lohmann, G. B. Raga, C. D. O'Dowd, M. Kulmala, S. Fuzzi, A. Reissell, and M. O. Andreae (2008), Flood or drought: How do aerosols affect precipitation?, *Science*, *321*(5894), 1309–1313.
Rotstayn, L. D., and U. Lohmann (2002), Tropical rainfall trends and the indirect aerosol effect, *J. Clim.*, *15*(15), 2103–2116.

Saleeby, S. M., S. R. Herbener, S. C. van den Heever, and T. L'Ecuyer (2015), Impacts of cloud droplet–nucleating aerosols on shallow tropical convection, *J. Atmos. Sci.*, *72*(4), 1369–1385.
Schneider, T., T. Bischoff, and G. H. Haug (2014), Migrations and dynamics of the Intertropical Convergence Zone, *Nature*, *513*(7516), 45–53.
Seifert, A., T. Heus, R. Pincus, and B. Stevens (2015), Large-eddy simulation of the transient and near-equilibrium behavior of precipitating shallow convection, *J. Adv. Model. Earth Syst.*, *7*, 1918–1937, doi:10.1002/2015MS000489.
Seigel, R. B. (2014), Shallow cumulus mixing and subcloud layer responses to variations in aerosol loading, *J. Atmos. Sci.*, doi:10.1175/JAS-D-13-0352.1.
Siebesma, A. P., C. S. Bretherton, A. Brown, A. Chlond, J. Cuxart, P. G. Duynkerke, H. Jiang, M. Khairoutdinov, D. Lewellen, and C. H. Moeng (2003), A large eddy simulation intercomparison study of shallow cumulus convection, *J. Atmos. Sci.*, *60*(10), 1201–1219.
Small, J. D., P. Y. Chuang, G. Feingold, and H. Jiang (2009), Can aerosol decrease cloud lifetime?, *Geophys. Res. Lett.*, *36*, L16806, doi:10.1029/2009GL038888.
Squires, P. (1958), The microstructure and colloidal stability of warm clouds, *Tellus*, *10*(2), 262–271.
Squires, P., and S. Twomey (1960), The relation between cloud droplet spectra and the spectrum of cloud nuclei, *Geophys. Monogr. Ser.*, *5*, 211–219.
Starr Malkus, J. (1954), Some results of a trade-cumulus cloud investigation, *J. Meteorol.*, *11*(3), 220–237.
Stevens, B. (2007), On the growth of layers of nonprecipitating cumulus convection, *J. Atmos. Sci.*, *64*(8), 2916–2931.
Stevens, B., and G. Feingold (2009), Untangling aerosol effects on clouds and precipitation in a buffered system, *Nature*, *461*(7264), 607–613.
Stevens, B., and R. Seifert (2008), Understanding macrophysical outcomes of microphysical choices in simulations of shallow cumulus convection, *J. Meteorol. Soc. Jpn.*, *86*, 143–162.
Takemi, T., O. Hirayama, and C. Liu (2004), Factors responsible for the vertical development of tropical oceanic cumulus convection, *Geophys. Res. Lett.*, *31*, L11109, doi:10.1029/2004GL020225.
Twomey, S. (1977), The influence of pollution on the shortwave albedo of clouds, *J. Atmos. Sci.*, *34*(7), 1149–1152.
Waite, M. L., and B. Khouider (2010), The deepening of tropical convection by congestus preconditioning, *J. Atmos. Sci.*, *67*(8), 2601–2615.
Walker, C. C., and T. Schneider (2006), Eddy influences on Hadley circulations: Simulations with an idealized GCM, *J. Atmos. Sci.*, *63*(12), 3333–3350.
Wang, C. (2004), A modeling study on the climate impacts of black carbon aerosols, *J. Geophys. Res.*, *109*, D03106, doi:10.1029/2003JD004084.
Wang, C. (2015), Anthropogenic aerosols and the distribution of past large-scale precipitation change, *Geophys. Res. Lett.*, *42*, 10,876–10,884, doi:10.1002/2015GL066416.
Warner, J., and S. Twomey (1967), The production of cloud nuclei by cane fires and the effect on cloud droplet concentration, *J. Atmos. Sci.*, *24*(6), 704–706.
Wu, P., N. Christidis, and P. Stott (2013), Anthropogenic impact on Earth's hydrological cycle, *Nat. Clim. Change*, *3*(9), 807–810.
Xue, H. W., and G. Feingold (2006), Large-eddy simulations of trade wind cumuli: Investigation of aerosol indirect effects, *J. Atmos. Sci.*, *63*(6), 1605–1622.
Xue, H. W., G. Feingold, and B. Stevens (2008), Aerosol effects on clouds, precipitation, and the organization of shallow cumulus convection, *J. Atmos. Sci.*, *65*(2), 392–406.
Yang, X., M. Ferrat, and Z. Li (2013), New evidence of orographic precipitation suppression by aerosols in central China, *Meteorol. Atmos. Phys.*, *119*(1-2), 17–29.
Yin, Y., Z. Levin, T. G. Reisin, and S. Tzivion (2000), The effects of giant cloud condensation nuclei on the development of precipitation in convective clouds—A numerical study, *Atmos. Res.*, *53*(1), 91–116.
Zhang, X., F. W. Zwiers, G. C. Hegerl, F. H. Lambert, N. P. Gillett, S. Solomon, P. A. Stott, and T. Nozawa (2007), Detection of human influence on twentieth-century precipitation trends, *Nature*, *448*(7152), 461–465.
Zhao, M., and P. H. Austin (2005), Life cycle of numerically simulated shallow cumulus clouds. Part I: Transport, *J. Atmos. Sci.*, *62*(5), 1269–1290.
Zuidema, P., Z. Li, R. J. Hill, L. Bariteau, B. Rilling, C. Fairall, W. A. Brewer, B. Albrecht, and J. Hare (2012), On trade wind cumulus cold pools, *J. Atmos. Sci.*, *69*(1), 258–280.